is a strong tendency for what might be called microstructural order; *i.e.* once a configuration of domains is established during the reaction, the boundaries between them will tend to take up directions and structures in which the discrepancies of phase and/or composition are accommodated with the maximum possible degree of local order. The elimination of all these boundaries will inevitably require very much more extensive migration of the contents of occupied tunnels, either *via* interstitial sites, or involving exchange with sites in the host lattice. In the case of $2Nb_2O_5.7WO_3$, this migration will be accompanied by the reorientation of elements of the host lattice, in order to produce the required arrangement of 4×4 ReO_3-type blocks. In view of these extensive movements, and the relatively weak long-range forces between occupied tunnels, these processes are likely to be slow, and it is therefore not surprising that large numbers of fault boundaries have been observed, particularly in $2Nb_2O_5.7WO_3$. These conclusions could probably be verified by examination of a series of specimens heat-treated for varying periods of time and/or varying temperature to demonstrate the method of approach to equilibrium.

One of us (S.I.) wishes to thank Professor J. M. Cowley for his continuous encouragement, and to acknowledge the support of a N.S.F. Area Development Grant in Solid State Science (No. GU 3169).

References

ALLPRESS, J. G. (1969*a*). *Mater. Res. Bull.* **4**, 707–720.
ALLPRESS, J. G. (1969*b*). *J. Solid State Chem.* **1**, 66–81.
ALLPRESS, J. G. (1972). In Natl. Bur. Stand. Spec. Publ. 364, *Solid State Chemistry. Proceedings of the 5th Materials Research Symposium.* Edited by R. S. ROTH and S. J. SCHNEIDER.
ALLPRESS, J. G., SANDERS, J. V. & WADSLEY, A. D. (1969). *Acta Cryst.* B**25**, 1156–1164.
ANDERSSON, S., MUMME, W. G. & WADSLEY, A. D. (1965). *Acta Cryst.* **21**, 802–808.
COWLEY, J. M. & IIJIMA, S. (1972). *Z. Naturforsch.* **27***a*, 445–451.
CRAIG, D. C. & STEPHENSON, N. C. (1969). *Acta Cryst.* B**25**, 2071–2083.
IIJIMA, S. (1971). *J. Appl. Phys.* **42**, 5891–5893.
IIJIMA, S. (1973). *Acta Cryst.* A**29**, 18–24.
IIJIMA, S. & ALLPRESS, J. G. (1973). *J. Solid State Chem.* **7**, 94–105.
IIJIMA, S. & ALLPRESS, J. G. (1974). *Acta Cryst.* A**30**, 29–36.
JAMIESON, P. B., ABRAHAMS, S. C. & BERNSTEIN, J. L. (1968). *J. Chem. Phys.* **48**, 5048–5057.
MAGNÉLI, A. (1949). *Ark. Kem.* **1**, 213–222.
O'KEEFE, M. A. (1973). *Acta Cryst.* A**29**, 389–401.
ROTH, R. S. & WADSLEY, A. D. (1965). *Acta Cryst.* **19**, 26–32.
ROTH, R. S. & WARING, J. L. (1966). *J. Res. Natl. Bur. Stand.* **70A**, 281–303.
SLEIGHT, A. W. (1966). *Acta Chem. Scand.* **20**, 1102–1112.
STEPHENSON, N. C. (1968). *Acta Cryst.* B**24**, 637–653.

Acta Cryst. (1974). A**30**, 29

Structural Studies by Electron Microscopy: Coherent Intergrowth of the ReO_3 and Tetragonal Tungsten Bronze Structure Types in the System Nb_2O_5–WO_3

BY S. IIJIMA*
Department of Physics, Arizona State University, Tempe, Arizona 85281, *U.S.A.*

AND J. G. ALLPRESS
Division of Tribophysics, CSIRO, University of Melbourne, Parkville, Victoria, 3052, *Australia*

(*Received* 4 *June* 1973; *accepted* 22 *June* 1973)

High-resolution lattice images from WO_3-rich compositions in the system Nb_2O_5–WO_3 contain direct evidence for the coherent intergrowth of extensive domains of several orientations of the ReO_3-type structure with the more complex tetragonal tungsten bronze-type structure. A model for the transformation between the two structure types is proposed.

1. Introduction

In a preceding paper (Iijima & Allpress, 1974), we have described high-resolution electron-optical observations of several phases in the system Nb_2O_5–WO_3, and shown how the direct correlation of image contrast with structural features can be used to derive reliable models for the structure of $2Nb_2O_5.7WO_3$, and of fault boundaries and intergrowths in this material and in $4Nb_2O_5.9WO_3$. The structure of $2Nb_2O_5.7WO_3$ can be regarded as an ordered intergrowth of minute domains of the ReO_3 and tetragonal tungsten bronze (TTB) structural types.

Some previous observations at lower resolution (Allpress, 1972*a*) revealed the occurrence of more extensive

* On leave from the Research Institute for Scientific Measurements, Tohoku University, Sendai, Japan.

coherent intergrowth of relatively large domains of $2Nb_2O_5.7WO_3$ with a second phase whose lattice was not resolved, in addition to the fault boundaries referred to above. On the basis of selected-area electron-diffraction data, it was concluded that the second phase was probably ReO_3-type, and a structural model for the intergrowth was proposed. We now wish to describe some high-resolution results which have been obtained from the same samples, and which confirm and considerably extend the earlier work.

2. Experimental

Samples having nominal $Nb_2O_5.WO_3$ molar ratios of 17:48, 1:3, 19:63, 3:7 and 2:7 were prepared and provided by Dr R. S. Roth and the late Dr A. D. Wadsley (Roth & Wadsley, 1965*a*; Roth & Waring, 1966). The techniques for specimen mounting for microscopy have been described previously (Iijima, 1973). The samples were examined at moderate resolution in a Philips EM200 microscope, and were found to be mixtures of varying proportions of the 4:9 and 2:7 phases, and in each case, a few fragments contained regions in which lattice fringes were not resolved. An example is shown in Fig. 1. The 17:48 and 19:63 samples were selected for further study at high resolution in a JEM 100B instrument, and lattice images were recorded from very thin (< 15 nm) fragments which were oriented so that the short (0·38 nm) *c* axis of the TTB-type host structure was aligned parallel to the incident electron beam. Focusing conditions were about 90 nm underfocus with respect to the Gaussian image plane.

3. Results

High-resolution lattice images from thin fragments which contain the structures which we wish to describe are reproduced in Figs. 2, 3, 4 and 5. A comparison of these images with those which we have presented previously (Iijima & Allpress, 1974) enables us to identify the contrast in the regions marked *A* (*A'*), *B* (*B'*) and *C* with the structures of $4Nb_2O_5.9WO_3$, $2Nb_2O_5.7WO_3$ and disordered TTB respectively. This contrast is directly related to the structures, in that white patches in the images correspond to empty tunnels of square and pentagonal cross section.

In addition to domains of these structures, the images contain regions marked *D* and *D'*, in which the matrix fringes form a square grid of spacing 0·38 nm. If we extend our contrast correlation to these regions, we must conclude that they have the ReO_3-type structure [Fig. 6(*a*)], in which metal–oxygen octahedra are joined by sharing corners in a cubic array, with $a = 0{\cdot}38$ nm. It can be seen clearly from Figs. 2 and 3 that when interfaced with domains of $2Nb_2O_5.7WO_3$ (*B*,*B'*), the ReO_3-type regions are oriented parallel to the 4×4 blocks of the same structure which lie in the central parts of unit cells of this phase.

In general, the ReO_3-type matrix itself contains a number of defects. A few isolated dark spots can be distinguished at *I* in Figs. 4 and 5(*a*). Larger square elements containing three white patches across a diagonal are marked *E* in Figs. 3, 4, and 5(*a*). Frequently, rows of similar elements were seen, lying parallel to $\langle 210 \rangle_R$ ($R = ReO_3$), as at *F*, and *F'* in Figs. 2 and 5(*a*). There are two possible orientations of the matrix (*D*, *D'*), and when these impinge as at *G* in Figs. 2(*b*) and 4, the boundaries contain distinctive contrast. Finally, the matrix is sometimes traversed by stepped faults, as at *H* in Fig. 5(*a*), which can be identified as crystallographic shear defects.

We will now proceed to make use of the observed contrast to derive possible models of these various structures. Most of them can be described in terms of a simple transformation between the ReO_3 and TTB structure types.

3.1 *Interstitial ions*

We believe that the dark spots marked *I* in Figs. 4 and 5(*a*) indicate the presence of interstitial metal ions lying in the tunnels between the corner-shared octahedra of the ReO_3 structure. These are the tunnels which, in the cubic tungsten bronzes, are occupied by alkali ions, and by *A* ions in ABX_3 compounds which possess the perovskite structure. The presence of these interstitial ions will effectively 'block' the corresponding tunnels, and lead to dark contrast in the image, rather than a white patch which is characteristic of an empty tunnel. We have no means of determining the occupancy of the blocked tunnels, but it seems quite probable that even a single interstitial ion would be sufficient to alter the image contrast from light to dark. Some experimental evidence to support this view is provided by recent observations of point defects in $Nb_{12}O_{29}$ (Iijima, Kimura & Goto, 1973).

3.2 *TTB Elements in a ReO_3-type matrix*

The groups of three white patches which lie across the square elements of contrast marked *E* in Figs. 3, 4 and 5(*a*) clearly correspond to similar groups which occur periodically in images from ordered $4Nb_2O_5.9WO_3$ and $2Nb_2O_5.7WO_3$, labelled *A* and *B* respectively in Figs. 2(*a*) and 3. In these structures, they are correlated with groups of four pentagonal tunnels surrounding a square tunnel in the TTB-type host lattice, two diagonally opposite tunnels being occupied. This arrangement is represented in the diagram in Fig. 6(*b*), and it is immediately obvious that it can be derived from the simpler ReO_3-type structure [Fig. 6(*a*)] by rotating the central four octahedra in Fig. 6(*a*) through 45°, and slightly distorting the outer octahedra.

The composition of the transformed elements is $M_9O_{27}(\text{octahedra}) + 2MO(\text{tunnels}) = M_{11}O_{29} = MO_{2{\cdot}636}$. They are therefore oxygen deficient with respect to WO_3, and are undoubtedly a consequence of the reaction with Nb_2O_5. The size of the elements of similar structure which occurs in $4Nb_2O_5.9WO_3$, is $1{\cdot}09 \times 1{\cdot}12$ nm, as determined from the atomic coor-

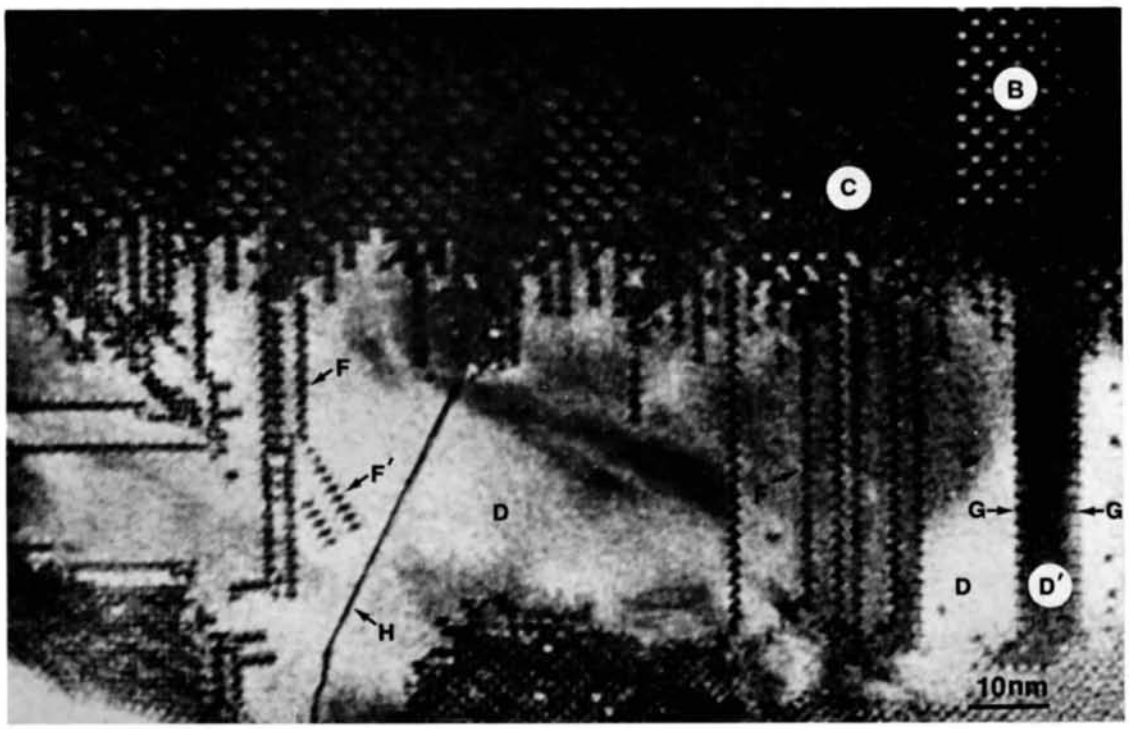

Fig. 1. Low-resolution lattice image from a fragment of nominal composition $17Nb_2O_5.48WO_3$, showing the intergrowth between a tetragonal bronze host lattice (containing domains *B* of $2Nb_2O_5.7WO_3$), and second unresolved structure labelled *D*. The features labelled *F*, *G* and *H* are identified by the high-resolution data as rows of TTB elements, orientation boundaries, and a crystallographic shear defect respectively.

[*To face p.* 30

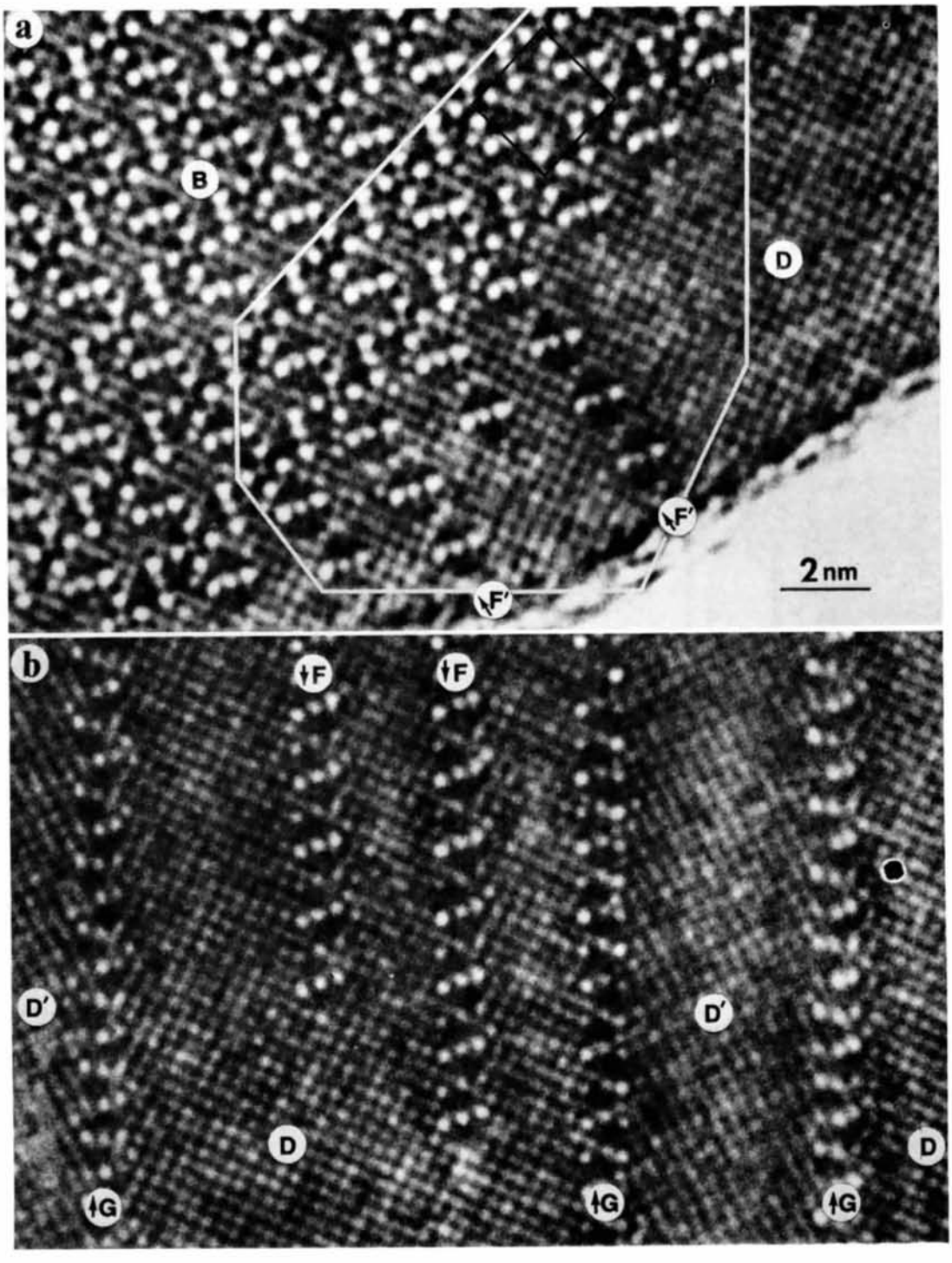

Fig. 2. (*a*) High-resolution lattice image, showing a domain of $2Nb_2O_5.7WO_3$ (*B*) intergrown with a region *D* of ReO_3-type structure. The arrows labelled *F'* indicate rows of TTB elements. The unit cell of $2Nb_2O_5.7WO_3$ is outlined by square. (*b*) High-resolution lattice image showing two orientations (*D*, *D'*) of the domains of ReO_3-type structure, which includes rows of TTB elements marked *F*. They are separated by reorientation boundaries marked *G*.

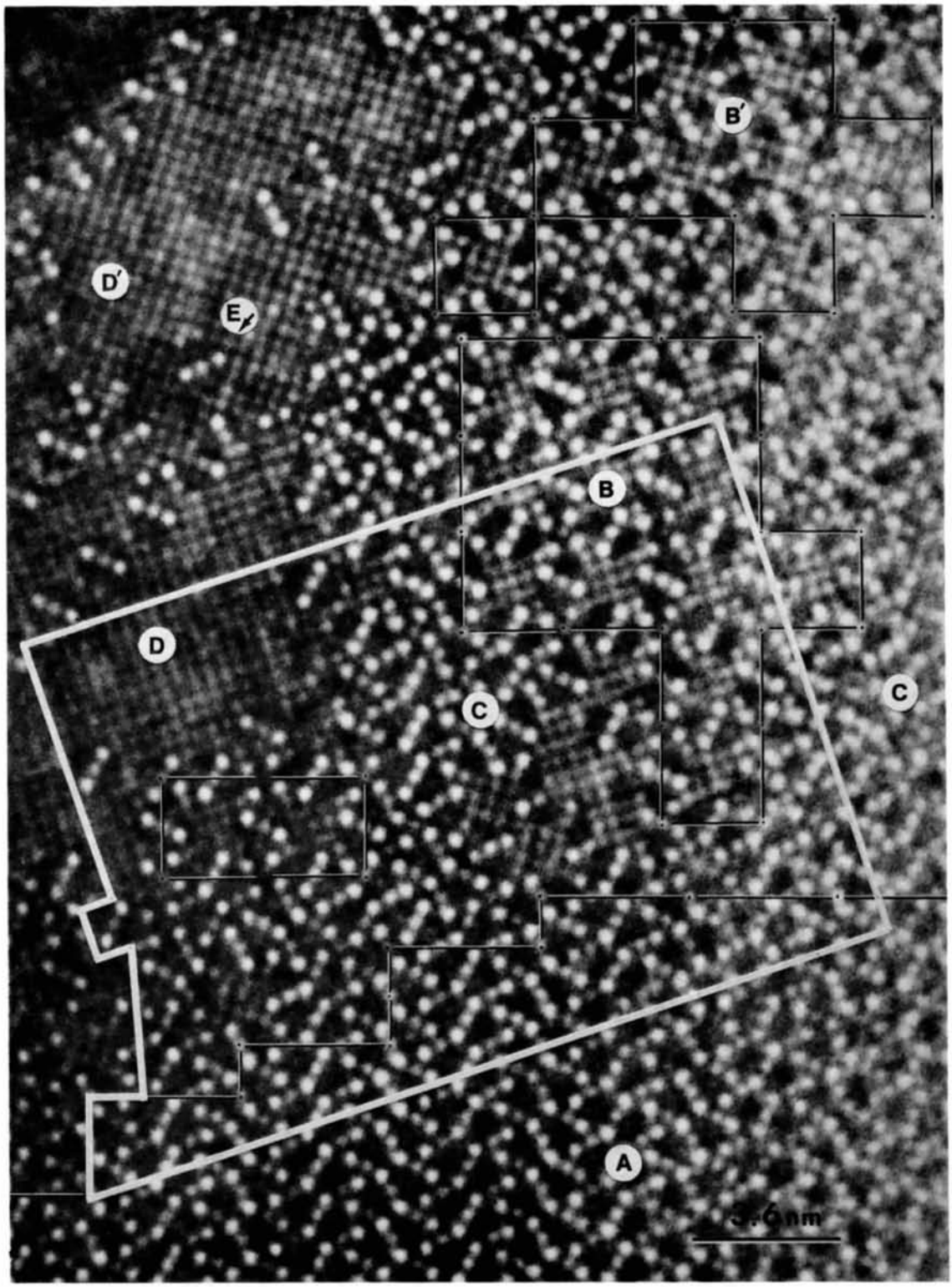

Fig. 3. Lattice image showing domains of $4Nb_2O_5.9WO_3$ (*A*), $2Nb_2O_5.7WO_3$ (*B*) and ReO_3-type structure (*D*, *D'*). Between these ordered regions, there are disordered regions of TTB structure (*C*).

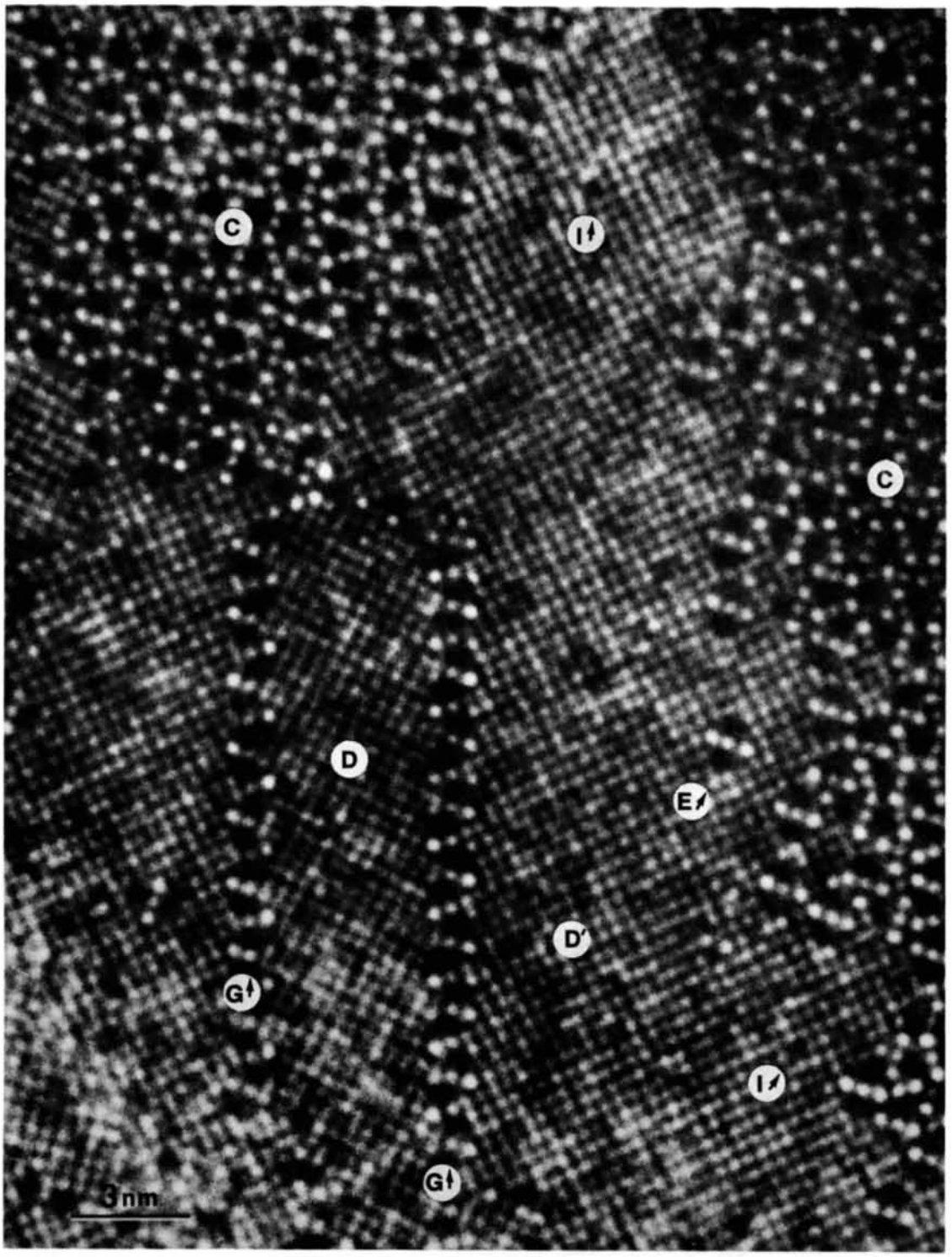

Fig. 4. Lattice image showing boundary regions of disordered regions of TTB structure (*C*) intergrown with regions of ReO_3-type structure (*D*). The regions of ReO_3-type structure contain point defects marked *I*, isolated TTB elements marked *E* and re-orientation boundaries marked *G*.

[*To face p.* 30

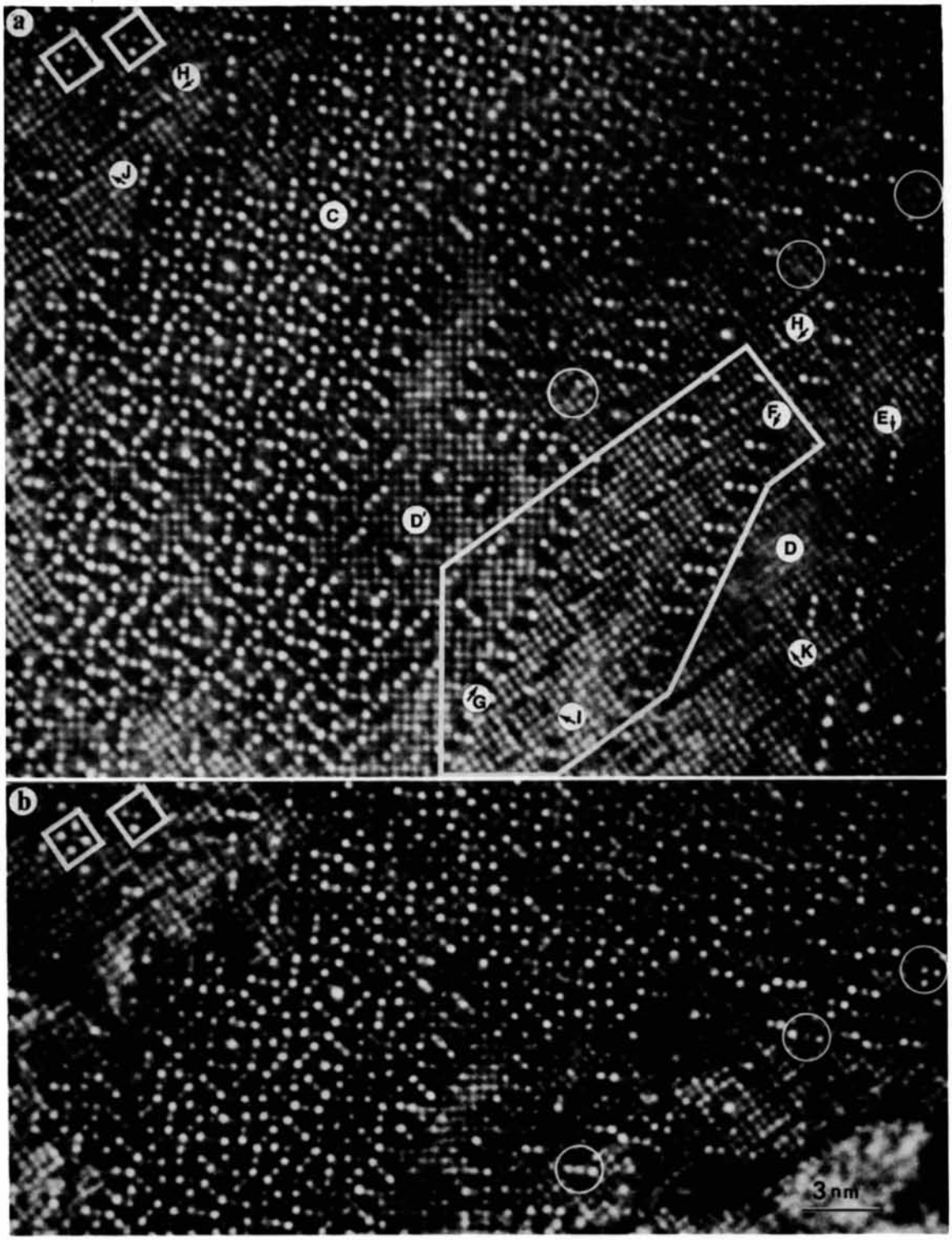

Fig. 5. (*a*) Lattice image showing boundary regions of disordered regions of TTB structure (*C*) intergrown with regions of ReO_3-type structure (*D*). The regions of ReO_3-type structure contain crystallographic shear planes marked *H*. The double-sized tunnels at the steps in a crystallographic shear plane are sometimes occupied at *J*. Terminated crystallographic shear plane is seen at *K*. (*b*) Image from the same region in (*a*) recorded after electron irradiation in the microscope. The circled regions of ReO_3-type material in (*a*) have been converted to TTB-type elements in (*b*). The occupancy of tunnels in the TTB elements enclosed by white squares in the top left corner is altered in (*b*). One element becomes completely unoccupied, and the other has a second tunnel occupied.

dinates given by Sleight (1966). This agrees closely with the size of the ReO_3-type element in Fig. 6(*a*); *i.e.* $3\times a=1{\cdot}14$ nm for $a=0{\cdot}38$ nm. Thus it seems clear that the transformed element can be accommodated satisfactorily in the ReO_3-type matrix with negligible strain.

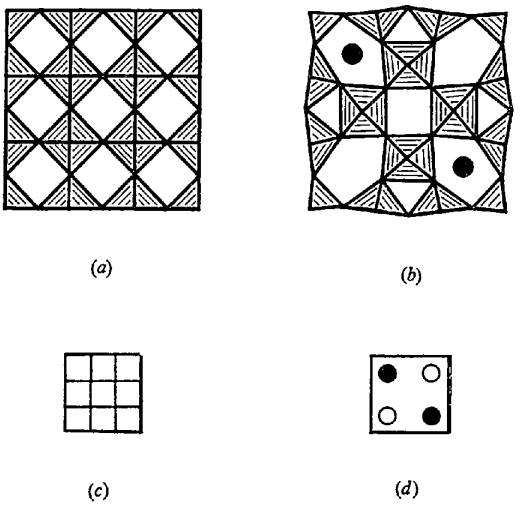

Fig. 6. (*a*) Idealized model of ReO_3-type structure, in which metal–oxygen octahedra are joined by sharing corners in a cubic array. (*b*) Model of TTB-type host structure, in which two diagonally opposite pentagonal tunnels are occupied by metal atoms (indicated by solid circles). (*c*) (*d*) Simpler representations of (*a*) and (*b*) respectively.

Rows of TTB elements, such as at F and F' in Figs. 2 and 5(*a*), are also easily incorporated in the matrix, as is shown in Fig. 7(*a*). Using the simpler representation of Fig. 6(*c*) and (*d*), they are also seen lying along $[1\bar{2}0]_R$ ($R=ReO_3$) in Fig. 7, and along $[2\bar{1}0]_R$ in Fig. 10, corresponding to the rows labelled F and F' in Figs. 2(*a*) and 5(*a*) respectively.

3.3 *TTB*-ReO_3 *boundaries*

The lattice image in Fig. 2(*a*) shows a boundary between a well ordered region of $2Nb_2O_5.7WO_3$ (*B*) and a domain of ReO_3-type structure (*D*), and the model in Fig. 7(*b*) shows the same boundary, together with the rows of TTB elements labelled F'. The model clearly shows the relationship between the unit cells in the two regions, with the axes of the TTB-type structure lying parallel to $[130]_R$ and $[\bar{1}30]_R$. The relationship between the cell dimensions can be obtained directly from the model; *i.e.* $a_T=(6^2+2^2)^{1/2}\times a_R=2{\cdot}4$ nm for $a_R=0{\cdot}38$ nm. This value is in satisfactory agreement with the experimental value of 2·43 nm (Roth & Waring, 1966).

The model in Fig. 8 shows the structure derived from the contrast in the enclosed area of Fig. 3, and illustrates a more complex situation where the boundary is rather poorly defined, and contains patches of ReO_3-type structure intergrown with relatively disordered TTB structure. Even in this case, the model was constructed almost entirely by converting square regions of the type shown in Fig. 6 from ReO_3 to TTB-type, according to the arrangement indicated by the image contrast. This simple procedure broke down in

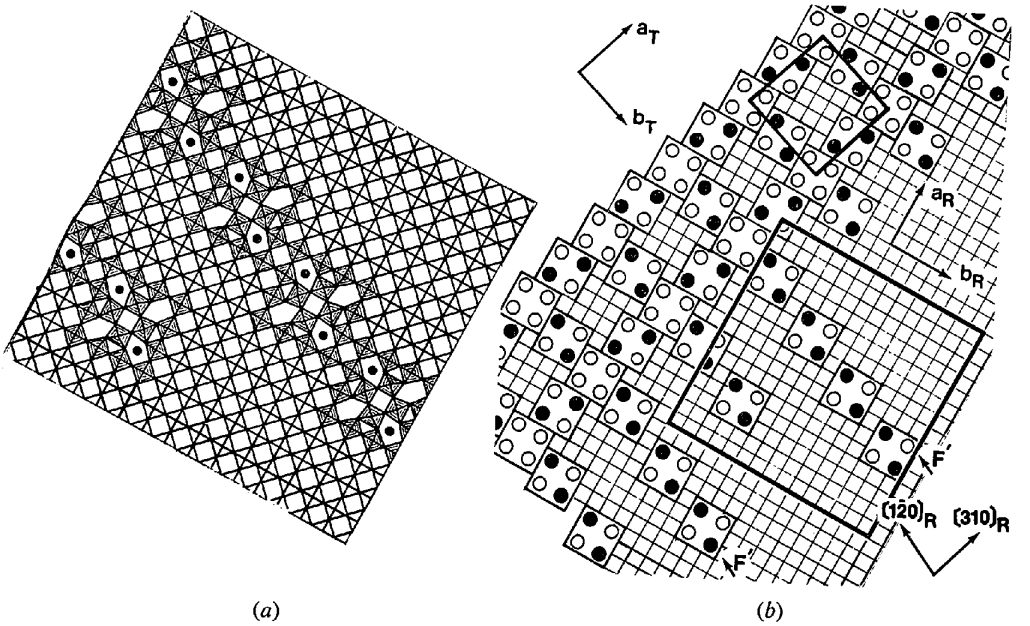

Fig. 7. (*a*) Idealized model of rows of TTB elements shown at F' in Fig. 2(*a*). TTB elements are coherently incorporated in the matrix of ReO_3 structure. (*b*) Simpler representation of the enclosed area in Fig. 2(*a*), showing a boundary of $2Nb_2O_5.7WO_3$ and ReO_3-type structure. The rows of TTB elements lie parallel to $[1\bar{2}0]_R$. The small square shows the unit cell of $2Nb_2O_5.7WO_3$. The enclosed area with a large square corresponds to the model in (*a*).

the areas marked by arrows, which will be referred to in more detail later.

It is obvious from these examples that the interface between the ReO_3 and TTB-type structures is coherent, and that both the boundary and the ordered TTB structures (*B* in Fig. 2, *A* and *B* in Fig. 3) can be derived from ReO_3 simply by the repeated application of the transformation which is illustrated in Fig. 6.

3.4 *Orientation boundaries*

Two orientations (*D*, *D'*) of the domains of ReO_3-type structure are evident in Figs. 2(*b*), 3, 4 and 5, and they are separated by boundaries marked *G*. An inspection of numerous micrographs confirmed that there is a fixed relationship between these orientations, such that the domains are rotated with respect to one another by 37° about [001]. This relationship is the same as that between the 4×4 ReO_3-type blocks in domains of $2Nb_2O_5.7WO_3$ (*e.g.* *B* and *B'* in Fig. 3) which are inverted with respect to each other. It arises from the fact that two TTB-type elements of the kind shown in Fig. 6(*b*) and (*d*) can be selected from a TTB lattice. They are outlined by full and dotted lines in Fig. 9(*a*), and at the right of this diagram, the corresponding ReO_3-type elements of the same size [Fig. 6(*a*) and (*c*)] are drawn. It is easy to show that the angle between the axes of the latter should be $\arctan\frac{3}{4} = 36°52'$.

The boundaries between these two orientations of ReO_3-type material [*G* in Figs. 2(*b*), 4 and 5] tend to lie parallel to $\langle 210\rangle_R$, and their image contrast is obviously closely related to that from the TTB-type regions. Their structure can be derived quite simply by extending the model in Fig. 9(*a*), as shown in Fig. 9(*b*). According to this model, the boundary consists of a row of interpenetrating TTB elements, which acts as a termination for the ReO_3-type structure on either side. A more detailed model of the same boundary is shown in Fig. 9(*c*).

It is clear that small patches of ReO_3-type structure in either of the two orientations described above can coexist within the TTB-type lattice, and this is illustrated in Fig. 3 and in the model in Fig. 8.

3.5 *Crystallographic shear defects*

It is well known that when WO_3 is reduced slightly, or doped with small amounts (10 mole %) of Nb_2O_5, its structure is modified by the presence of crystallographic shear defects, along which neighbouring octahedra share edges rather than corners. In ordered materials such as $W_{20}O_{58}$ (Magnéli, 1950), they are planar and regularly spaced, and their structure is known from X-ray studies. In the Nb_2O_5–WO_3 system, they tend to be unequally spaced, and to change direction as they traverse the ReO_3-type matrix (Allpress, 1972*b*, Bursill & Hyde, 1972*a*). Their structure has been inferred from electron-optical observations at low resolution, and by extrapolation from the X-ray determinations of ordered structures.

The presence of crystallographic shear defects within ReO_3-type domains intergrown with TTB structures was suspected during a previous low-resolution study (Allpress, 1972*a*); the line marked *H* in Fig. 1 being the only kind of evidence which was obtained at that time. The higher resolution of the present observations has enabled us to obtain much more direct evidence of the presence and structure of defects of this kind. A number of examples of contrast which we believe to be due to these defects can be seen in Fig. 5(*a*), particularly along the directions marked *H*. The contrast consists of stepped dark bands, across which the fringes typical of the ReO_3-type lattice are displaced by about half their normal spacing. Most of the steps contain a white patch which is larger and elongated compared with those in the surrounding matrix.

Fig. 10 shows a model of the area enclosed in Fig. 5(*a*), which includes a crystallographic shear defect *H*,

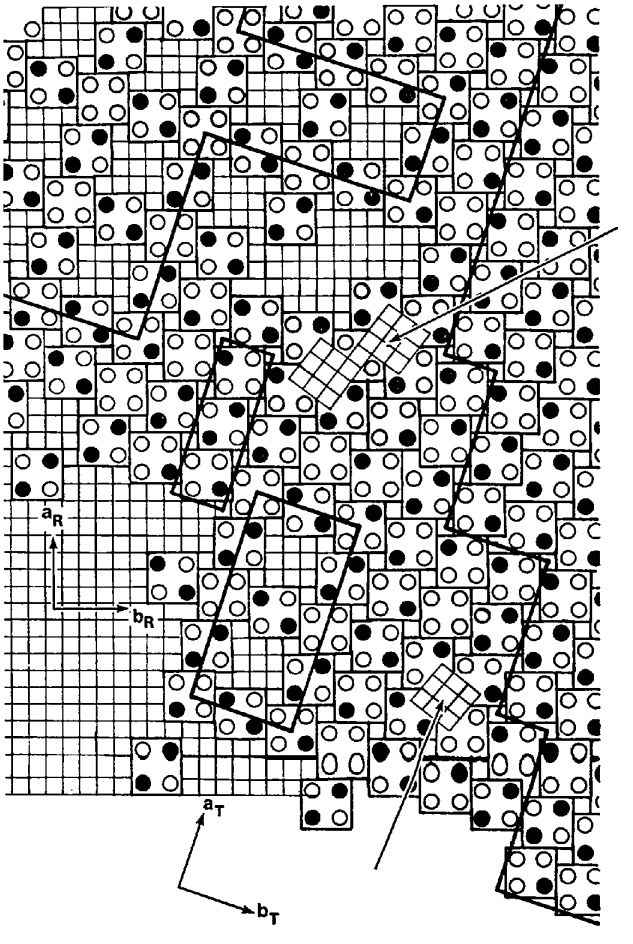

Fig. 8. Model of the enclosed area in Fig. 3, showing more complex region including patches of ReO_3-type structure intergrown with regions of disordered TTB structure, ordered $4Nb_2O_5.9WO_3$ and $2Nb_2O_5.7WO_3$ (enclosed with thick lines), but they are coherently intergrown. The model was constructed by converting square regions of the type shown in Fig. 6 from ReO_3 to TTB-type.

lying between a row of TTB-type elements F and a reorientation boundary G. Its average orientation lies between $[3\bar{1}0]_R$ and $[2\bar{1}0]_R$, both these directions being known for crystallographic shear planes in ordered structures. Individual octahedra are outlined along several sections of the defect, and the model indicates that they share edges along the straight portions, and leave double-sized tunnels parallel to $\mathbf{c}_R$ at the steps. Both these features are in keeping with the observed contrast, thick dark lines where octahedra share edges and larger white patches at the steps. Also, the observed displacement of the fringes as they cross the defect is reproduced satisfactorily.

The model is consistent with the structures of crystallographic shear planes determined from X-ray studies of ordered crystals, and confirms in detail the structures proposed previously for non-planar defects in WO_3 doped with Nb_2O_5 (Allpress, 1972*b*). However, there is evidence in the present observations that the double-sized tunnels may sometimes be occupied, since the larger patches of white contrast are missing from several of the steps, such as at J in Fig. 5(*a*). Occupied tunnels with similar geometry are known in ordered structures, such as $NaNb_{13}O_{33}$ (Andersson, 1965).

Several of the defects in Fig. 5(*a*) are terminated within the crystal, *e.g.* at K. It is not possible to make a model of such a termination without some distortion of the lattice, and we suspect that slightly wider-than-normal dark lines in the vicinity of the terminations may indicate that this distortion is accommodated over a region 1–2 nm in diameter. A model for such a termination dislocation has been proposed (Allpress, Tilley & Sienko, 1971), but further high-resolution observations will be required before it can be checked satisfactorily.

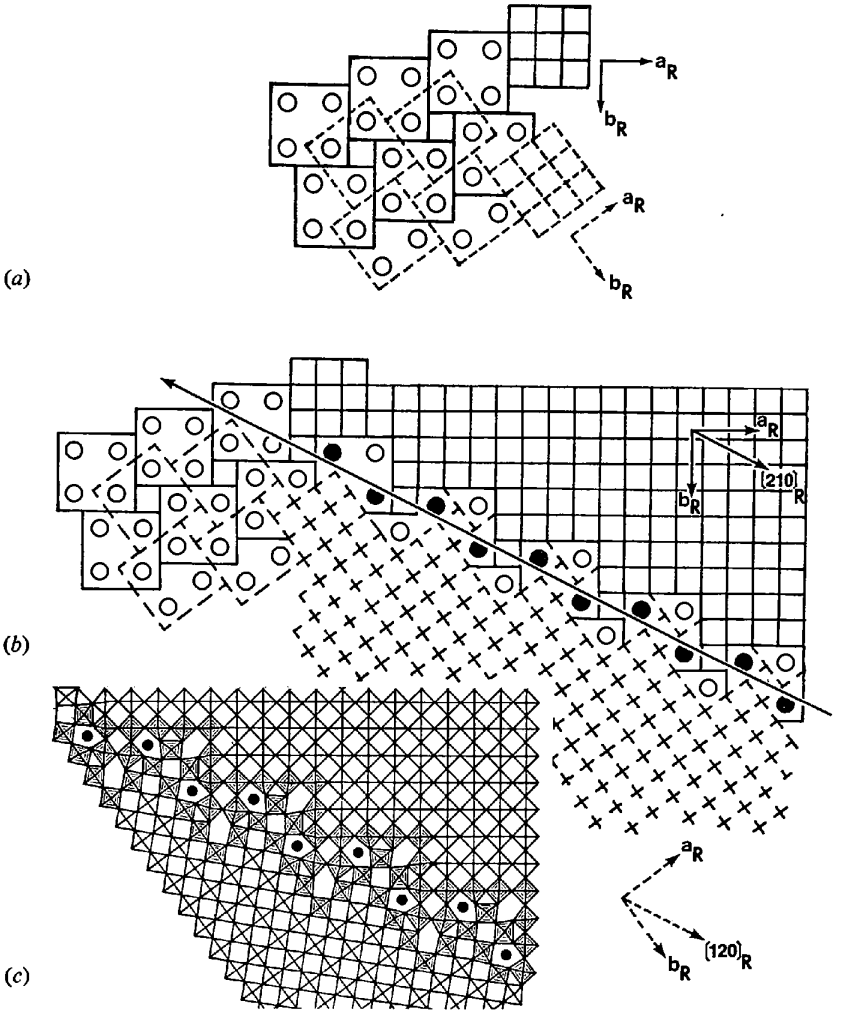

Fig. 9. (*a*) Model showing two TTB-type elements selected from a TTB lattice and at the right, the corresponding ReO_3-type elements are shown. (*b*) Representation of the boundary between two orientations of ReO_3-type material shown at G in Figs. 2(*b*), 4 and 5, which lies parallel to $[210]_R$. The boundary consists of a row of interpenetrating TTB elements shown in (*a*). (*c*) Detailed model of the same boundary shown in (*b*).

3.6 *In situ observations of structural changes*

The results which have been presented already have been interpreted in terms of a structural model which is based on the transformation of a 4×4 block of ReO_3-type material to a TTB element of the same size (Fig. 6). Associated with this transformation in the host structure is the insertion of additional metal and oxygen into pentagonal tunnels in the TTB element. Such a sequence of events could form the basis for a plausible mechanism for the reaction of Nb_2O_5 with WO_3, and we therefore attempted to obtain more direct evidence by looking for changes of contrast in images recorded from thin fragments before and after short periods of intense electron bombardment in the microscope. A pair of such images is reproduced in Fig. 5. The experiment is difficult, and the results must be treated with caution, because in addition to heating the fragment the procedure also obviously involves bombardment by energetic electrons and build-up of contamination on the specimen; nevertheless we believe that the results are significant. An examination of the contrast in Fig. 5 shows that the circled regions of ReO_3-type material in (*a*) have been converted to TTB-type in (*b*). In most cases, the TTB elements have two diagonally opposite pentagonal tunnels occupied, but in the top right-hand circle, the contrast indicates that two adjacent are tunnels occupied. In addition, the occupancy of tunnels in the two TTB elements enclosed by squares in the top left-hand corner of Fig. 5(*a*) is altered in (*b*). One element becomes completely unoc-

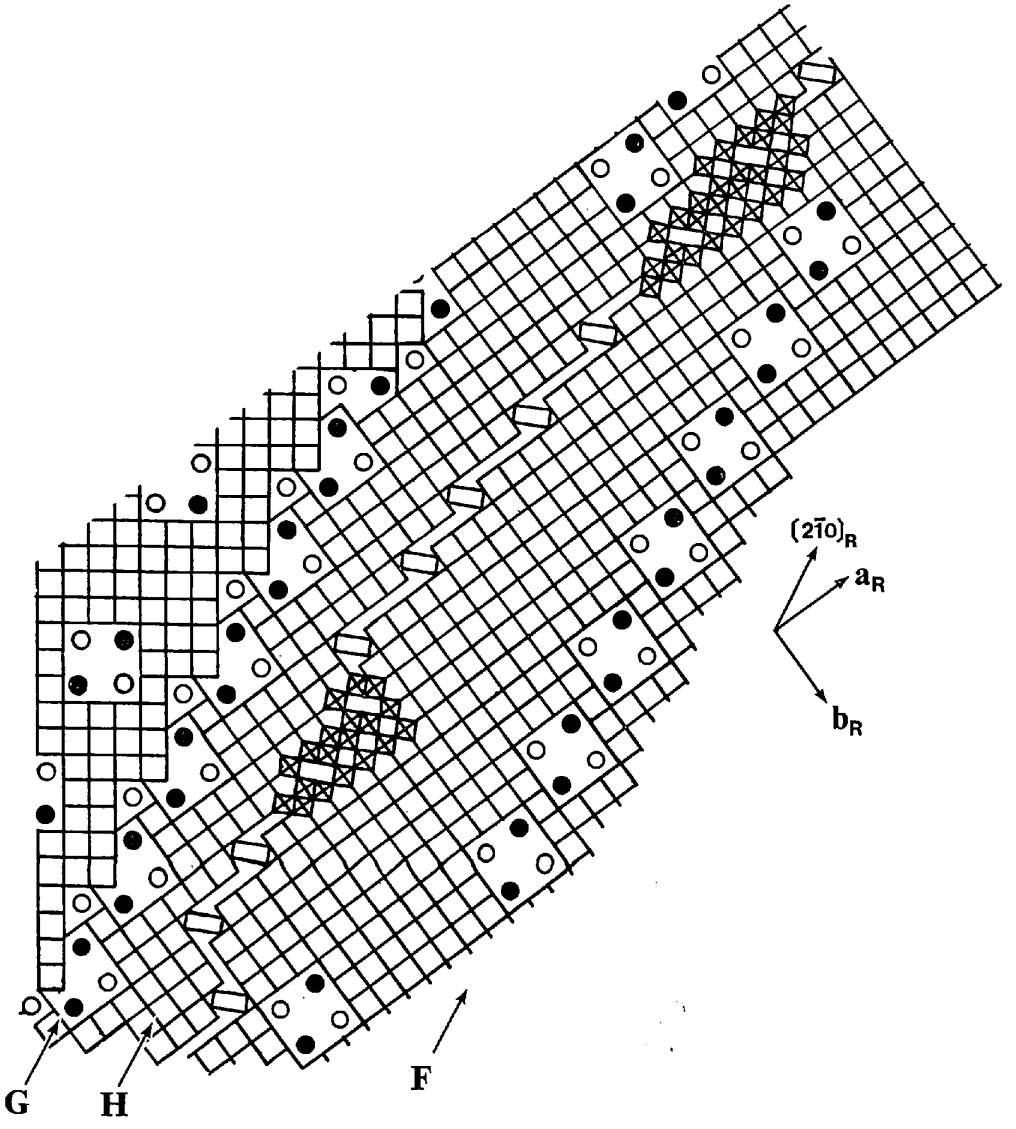

Fig. 10. Model of the enclosed area in Fig. 5(*a*), showing a crystallographic shear defect *H*, lying between a row of TTB-type elements *F* and a reorientation boundary *G*. Its average orientation lies between $[3\bar{1}0]_R$ and $[2\bar{1}0]_R$. Individual octahedra are outlined along several sections of the defect, and leave double-sized tunnels parallel to c_R at the steps.

cupied, and the other has a second tunnel occupied.

These observations tend to support the view that the transformation illustrated in Fig. 6 is involved in the reaction, and that migration of ions between pentagonal tunnels is a possible diffusive process.

4. Discussion

4.1 *Structure determination*

We have presented models for a variety of disordered structures, which were derived by assuming a direct correlation between contrast in high-resolution lattice images and structural features, particularly unoccupied square and pentagonal tunnels. These correlations were justified previously (Iijima, 1971; Iijima & Allpress, 1973, 1974) by observing the contrast in images from ordered samples of related and known structure, and we have been careful to reproduce the appropriate experimental conditions of orientation, defect of focus, and crystal thickness as far as possible in the present work. We are confident that the results are reliable, and they demonstrate the value of the technique of lattice imaging for the detailed study of disordered materials.

The present work largely confirms models for crystallographic shear defects, reorientation boundaries, and interfaces between TTB and ReO_3-type structures, which were proposed following previous studies at lower resolution (Allpress, 1972*a*,*b*). In addition, they provide direct evidence for the presence of interstitial ions, individual TTB elements, and for the occupancy of pentagonal tunnels, which was not available before. In the absence of the electron-optical results, it seems unlikely that intergrowth of the two structure types would have been suspected.

4.2 *Structure and stoichiometry*

The system Nb_2O_5–WO_3 illustrates the great versatility with which the ReO_3 structure type can accommodate itself to changes in composition. At both ends of the range of oxygen–metal ratios (O/M), this is achieved by the insertion of crystallographic shear planes, either in one direction in the Magnéli phases ($O/M = 2{\cdot}9$–$3{\cdot}0$, Allpress, 1972*a*) or in two in the block structures related to Nb_2O_5 ($O/M = 2{\cdot}5$–$2{\cdot}66$, Roth & Wadsley, 1965*b*; Allpress, Sanders & Wadsley, 1969). In both cases, the unaltered regions of the ReO_3-type matrix can be clearly distinguished, either as blocks or slabs extending through the structures. At intermediate compositions ($O/M = 2{\cdot}74$–$2{\cdot}82$) the crystallographic shear structures are replaced by a series of TTB-type structures, which are related to ReO_3 by a rotation of octahedra rather than a shear, as is indicated in Fig. 6. This rotation is accompanied by the formation of larger pentagonal tunnels, which can accommodate additional strings of metal and oxygen atoms, thus allowing the oxygen–metal ratio to vary below 3·0.

The role and behaviour of the TTB elements appears to be quite similar to those of crystallographic shear defects. Both provide a means of accommodating non-stoichiometry, and both may occur either as isolated defects in a WO_3 matrix, or as disordered groups, or as recognizable structural entities in well characterized phases. In principle, it would be possible to cover the whole range of oxygen–metal ratios from 3·0 down to 2·5 and lower by steadily increasing the number of either of these defects. However, it is clear that the energies of both configurations will vary with composition, and this is the most likely reason for the observed changes in structure type across the phase diagram.

In a recent communication, Bursill & Hyde (1972) have introduced the concept of rotation faults, and used this to derive the relationship between the ReO_3 and TTB structure types (Fig. 6). The TTB elements which we have observed [Figs. 3 and 5(*a*)] are examples of these rotation faults, and provide direct experimental evidence to support their proposed models.

4.3 *The reaction mechanism*

Each of the samples which we have studied has proved to be a mixture of several phases, present either as separate faulted crystals or intergrown in a variety of complex ways. The departure from equilibrium which is indicated by these results appears to have two possible sources:

(*a*) The high-temperature situation has not been retained during the quenching procedure [the samples were prepared in sealed platinum capsules at 1620°K, and quenched by dropping from the furnace into water (Roth & Wadsley, 1965*a*)].

(*b*) Complete reaction was not achieved during the period of heating (18 h) at 1620°K.

Since many fragments were comparatively well ordered over quite large areas [*e.g.* the regions *B* in Fig. 2(*a*) and *A* in Fig. 3 extended well beyond the borders of these figures], we are inclined to believe that the quenching treatment was successful, and that the reaction of the powdered mixture of oxides was incomplete. If this is the case, the observed disordered regions may be regarded as areas where reaction is incomplete, and the quenched-in structure might yield clues as to the mechanism by which the ordered TTB structures are built up.

We have already used the concept of the rotation of octahedra to illustrate the conversion of elements of ReO_3 to TTB-type structure (Fig. 6). A mechanism for the formation and growth of such a rotation fault has been proposed by Bursill & Hyde (1972*a*,*b*). The case of the growth of a tetragonal bronze M_xWO_3 by reaction of WO_3 with metal vapour is attractively simple: one can envisage the penetration of metal ions into interstitial sites until at some critical concentration, the energy of the system will be reduced by the rotation of octahedra (Fig. 6) and occupation of the larger pentagonal tunnels by migration of interstitials. A similar mechanism for the reaction of Nb_2O_5 with a host matrix of WO_3 is unsatisfactory in several respects. Firstly, WO_3 has a vapour pressure of the order of 1 torr at the reaction

temperature (1620°K) (Blackburn, Hoch & Johnston, 1958), and it is therefore unlikely to be the host structure under these conditions. Secondly, the stoichiometry of the system requires that Nb_2O_5 must contribute to the host lattice as well as filling tunnels. Since the host lattice composition is MO_3, that of the tunnels is MO, and that of Nb_2O_5 can be written as $\frac{1}{2}(3NbO_3.NbO)$, it is evident that only 25% of the niobium can be accommodated in the tunnels: the remainder must be used to extend the host lattice.

Because of the volatility of WO_3, it is probably more realistic to assume that Nb_2O_5 is the immobile species, and that reaction will proceed by vapour transport of WO_3 on to the surface of the block structures related to the high-temperature form of Nb_2O_5 (Roth & Wadsley, 1965*a*,*b*). Kinetic experiments on the analogous MoO_3–Nb_2O_5 reaction (Andersson, 1969) indicate that formation of these phases occurs rapidly when the vapour pressure of the trioxide is of the order of 1 torr. As the WO_3 content of the product increases, so will the size of the component blocks, until finally the Nb_2O_5-type of structure loses stability, and transformation to WNb_2O_8 occurs. The structure of the latter (Lundberg, 1972) is closely related to that of $LiNb_6O_{15}F$ (Lundberg, 1965), which as Hyde & O'Keeffe (1973) have shown, can be readily derived from the ReO_3 structure by the periodic application of the rotation operation illustrated in Fig. 6. This implies that WNb_2O_8 can probably transform readily to the TTB-type structures and can also form intergrowths with the ReO_3-type lattice of WO_3, as further WO_3 becomes available for reaction. In fact, one can envisage the topotaxic growth of condensing WO_3 vapour on any of these phases, followed by diffusion in the solid state to form a homogeneous product.

We believe that the inhomogeneities which we have found in individual fragments, as illustrated by the micrographs which are reproduced in this paper, arise as a consequence of fluctuations in the supply of WO_3 to the growing crystals in the early stages of the reaction. These fluctuations are probably caused by changes in the flux of WO_3 vapour within the tightly packed mixture of oxides, due to the opening and closing of paths for diffusing vapour as WO_3 is consumed and crystals of the product grow. Because of the close crystallographic relationships between the growing phases and WO_3, it is quite possible, for example, for a WO_3-rich domain to grow on to a crystal, and subsequently be 'buried' by further growth of product, or contact with an adjacent crystal. Once such a domain is buried within a crystal, it can only disappear by solid-state diffusion in the same crystal, leading finally to one or more phases, in each of which the distribution of TTB elements is uniform. It appears that this stage of the process is slow, and probably not particularly rewarding in terms of a reduction in energy, since the domain boundaries are coherent and therefore of low energy. For these reasons, the grown-in inhomogeneities tend to persist.

Within the domains themselves, microstructural order can be established rather more rapidly. The migration of TTB elements is easily achieved *via* diffusion of interstitials and the rotation of octahedra in the host matrix. Confirmation of this type of mechanism is provided by the *in situ* observation of structural changes (Fig. 5). It seems likely that rows of TTB elements [*F* and *F'* in Figs. 2(*b*), 4 and 5] and reorientation boundaries (*G* in Figs. 4 and 5) are extended defects which form during the early stages of the annealing process, and tend to minimize the energy at a local or microstructural level.

We have benefited from stimulating discussions with Drs M. O'Keeffe and H. J. Rossell. One of us (S.I.) wishes to thank Professor J. M. Cowley for his continuous encouragement, and to acknowledge the support of a N.S.F. Area Development Grant in Solid State Science (No. GU3169).

References

ALLPRESS, J. G. (1972*a*). Natl. Bur. Stand. Spec. Pub. 364, *Solid State Chemistry, Proceedings of 5th Materials Research Symposium.* Edited by R. S. ROTH and S. J. SCHNEIDER.

ALLPRESS, J. G. (1972*b*) *J. Solid State Chem.* **4**, 173–185.

ALLPRESS, J. G., SANDERS, J. V. & WADSLEY, A. D. (1969). *Acta Cryst.* B**25**, 1156–1164.

ALLPRESS, J. G., TILLEY, R. J. D. & SIENKO, M. J. (1971). *J. Solid State Chem.* **3**, 440–451.

ANDERSSON, S. (1965). *Acta Chem. Scand.* **19**, 557–563.

ANDERSSON, S. (1969). *Z. anorg. allgem. Chem.* **366**, 96–103.

BLACKBURN, P. E., HOCH, M. & JOHNSTON, H. L. (1958). *J. Phys. Chem.* **62**, 767–773.

BURSILL, L. A. & HYDE, B. G. (1972*a*). *J. Solid State Chem.* **4**, 430–446.

BURSILL, L. A. & HYDE, B. G. (1972*b*). *Nature Phys. Sci.* **240**, 122–124.

HYDE, B. G. & O'KEEFFE, M. (1973). *Acta Cryst.* A**29**, 243–248.

IIJIMA, S. (1971). *J. Appl. Phys.* **42**, 5891–5893.

IIJIMA, S. (1973). *Acta Cryst.* A**29**, 18–24.

IIJIMA, S. & ALLPRESS, J. G. (1973). *J. Solid State Chem.* **7**, 94–105.

IIJIMA, S. & ALLPRESS, J. G. (1974). *Acta Cryst.* A**30**, 22–29.

IIJIMA, S., KIMURA, S. & GOTO, M. (1973). *Acta Cryst.* A**29**, 632–636.

LUNDBERG, M. (1965). *Acta Chem. Scand.* **19**, 2274–2284.

LUNDBERG, M. (1972). *Acta Chem. Scand.* **26**, 2932–2940.

MAGNÉLI, A. (1950). *Ark. Kem.* **1**, 513–523.

ROTH, R. S. & WADSLEY, A. D. (1965*a*). *Acta Cryst.* **19**, 26–32.

ROTH, R. S. & WADSLEY, A. D. (1965*b*). *Acta Cryst.* **19**, 42–47.

ROTH, R. S. & WARING, J. L. (1966). *J. Res. Natl. Bur. Stand.* **70**A, 281–303.

SLEIGHT, A. W. (1966). *Acta Chem. Scand.* **20**, 1102–1112.